

THIRTEENTH EUROPEAN ROTORCRAFT FORUM

2.12

Paper No. 37

**COMPARISON WITH FLIGHT DATA OF HOVER PERFORMANCE
USING VARIOUS ROTOR WAKE MODELS**

K. R. REDDY, N. E. GILBERT

AERONAUTICAL RESEARCH LABORATORIES
MELBOURNE, AUSTRALIA

September 8-11, 1987

ARLES, FRANCE

COMPARISON WITH FLIGHT DATA OF HOVER PERFORMANCE USING VARIOUS ROTOR WAKE MODELS

K. R. Reddy, N. E. Gilbert

Aeronautical Research Laboratories
Melbourne, Australia

Abstract

Three nonuniform inflow rotor wake models and a uniform inflow model based on momentum theory are used to compare predicted hover performance with flight data for four helicopters. Comparisons are also made of blade loading distribution for one of these. Two of the nonuniform inflow models use a prescribed wake geometry based on model rotor flow visualization studies, representing vortices by a helical lattice of finite length straight-line elements in one case, and by infinite and semi-infinite straight lines in the other. A free wake geometry is used for the remaining model, with line vortices generally represented by rings. To investigate the consistency of these methods, the same parameters and empirical corrections are used within each model in applying to each helicopter, and where possible, consistency of appropriate quantities between models is also maintained. It is shown that while consistently good estimates of hover performance are given by the uniform inflow method using the same induced velocity factor for all cases, good estimates are only given by the nonuniform inflow methods if certain parameters are adjusted individually for each case. However, intermediate results, such as blade loading distribution, are given more accurately by the latter methods. For the genuine prediction problem, where test data is unavailable, a strategy is suggested where both uniform and nonuniform methods are used together.

1. INTRODUCTION

Aeronautical Research Laboratories (ARL) presently has an analysis capability in the area of hovering rotor aerodynamics which includes codes both developed inhouse and acquired from outside. At ARL in the late 1970's and early 1980's, Reddy developed a prescribed wake method for hover using infinite and semi-infinite straight-line vortices¹ that was done independently of very similar work by Miller² at Massachusetts Institute of Technology (MIT) and Beddoes (unpublished) at Westland Helicopters Limited (WHL). The work was targetted at developing a computationally efficient method for inclusion within the Sea King simulation model at ARL.³ Following requests from the Australian Services to evaluate performance characteristics, especially for hover, of helicopters being considered for procurement, ARL has developed its own specialized closed form solution codes based on momentum theory⁴ and, more recently, has extended Reddy's vortex line method.⁵

In 1984, as part of a cooperative program with the US Army Laboratories, ARL was able to acquire CAMRAD (Comprehensive Analytical Model of Rotorcraft Aerodynamics and Dynamics), which was developed by Johnson⁶⁻⁹ at Ames Research Center. The code uses straight-line vortex elements joined in the form of a helical vortex lattice to represent the trailed and shed vorticity. The wake geometry models include simple undistorted models, prescribed wake models for hover that are based on the experimental data of Landgrebe¹⁰ and Kocurek and Tangler¹¹, and a free wake model for forward flight. In 1985, a free wake hover code using vortex rings was acquired and subsequently implemented at ARL, the code being based on one of the variations in Miller's method.²

Comprehensive codes such as CAMRAD allow the analysis of a complete rotorcraft, usually allowing for two separate rotors. However, for the hover performance analysis of a conventional helicopter with a single main rotor and anti-torque tail rotor, it is assumed sufficient to consider only the main rotor. Standard estimates are then made for the power requirements of the

tail rotor, accessories and transmission, and aerodynamic interference. By assuming an axisymmetric wake, the harmonics of blade motion and the shed wake can be neglected, and only collective control needs to be adjusted to trim to a specified thrust.

Given the problem of estimating hover performance of a rotor for which experimental data are not available to the analyst, the question that arises is how can each of the methods at the analyst's disposal best be used, and are there significant differences in reliability of the methods. In 1974, Ormiston¹² coopted several rotor loads specialists to undertake a project which involved each one using their own code to predict helicopter rotor loads for a hypothetical helicopter rotor at three forward flight conditions. However, the hover case was not included and the investigations focused on the prediction of rotor forces, moments, and blade flapping. More recently, in 1987, Harris¹³ presented a review on rotary wing aerodynamics which included a discussion of hover performance predictions, pointing to the inadequacies of predictions that was to some extent demonstrated earlier in 1980 by Kocurek et al.¹⁴ However, though predictions were compared for a range of experimental data, only the prediction methodology developed at Bell Helicopter Textron (BHT) was used in Refs. 13 and 14.

The main purpose of this paper then is to investigate the consistency of different methods in predicting hover performance. Primary interest is focused on the various wake models which provide realistic nonuniform rotor inflow. Though the uniform inflow solution based on momentum theory does not provide a realistic blade load distribution, total power estimates have traditionally been found to correlate well with experimental data, after allowing for certain corrections. In assessing the nonuniform inflow methods therefore, the uniform inflow predictions, obtained using CAMRAD, are also included. Comparisons are given with available test data for a number of helicopters using the same empirical corrections within each model. Where possible, consistency of appropriate quantities between models is also maintained. Such a study is of course limited by the availability to us of test data together with appropriate input data to drive the models and to the availability of the models themselves. Hover performance estimates of main rotor power as a function of thrust are compared with test data for the Bell UH-1H Iroquois, Aérospatiale AS-350B Squirrel, Westland Wessex, and Sikorsky CH-53A Sea Stallion. Comparisons are also made of blade loading as a function of radius for the Sikorsky S-58 (equivalent to Wessex). The wake models used are:

- Helical vortex lattice prescribed wake model based on Kocurek and Tangler geometry (in CAMRAD)
- Vortex line prescribed wake model by Reddy at ARL
- Vortex ring free wake model by Miller at MIT

2. WAKE MODELS

There have been many attempts to develop three-dimensional computational models with the basic vortex elements appearing in Gray's¹⁵ schematic representation of experimental results (see Fig. 1). Because blade lift and circulation are concentrated at the tip, the strength of the trailing vorticity is high at the outer edge of the rotor wake. The vorticity rolls up into a strong concentrated tip vortex, which is well represented by line elements. Since the gradient of bound circulation inboard of the blade tip is low, the inboard vorticity is much weaker and more diffuse than at the tip and there are many variations in its representation (Ref. 16, Chapt. 13).

The common approach has been to develop models that closely trace the three-dimensional helical shape of both the strong tip vortex and inboard vortex sheet shown in Fig. 1. Unfortunately, this apparently straight-forward approach results in a computation process that is complex and computationally demanding. This is especially so for the hover case where there is no large uniform relative wind due to the translational velocity of the helicopter. This means that

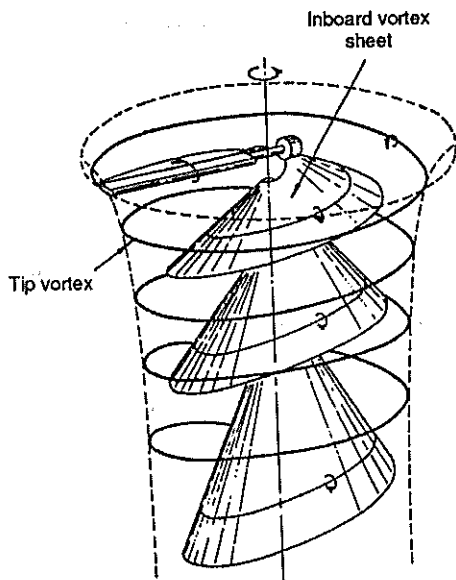


Fig. 1 Hovering rotor wake structure

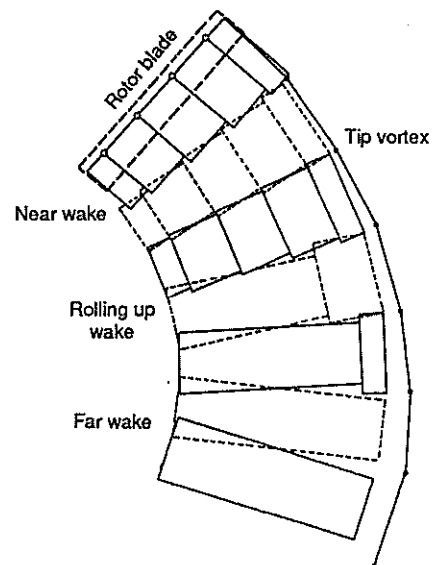


Fig. 2 Helical vortex lattice wake model

the wake is not swept away from the rotor and hence more of the wake must be considered. It also means that wake induced velocities are the only velocities present, resulting in a greater sensitivity of the wake geometry to changes in induced velocity. This increased sensitivity leads to instabilities and slow wake convergence if free wake models are used.¹⁷

In an attempt to overcome the above problems, there has been some interest on methods of simplifying the helical representation for the hover case.^{2,5,18} The two such axisymmetric methods used here are similar in that the continuously descending helix is represented by vertically separated horizontal vortex lines (for a horizontal rotor disc), which are either straight or circular.

If the distribution of vorticity in the wake is known, then the velocity at any point can be calculated using the Biot-Savart law. According to this law, the induced velocity at a point varies inversely with the square of its distance from a finite vortex element. Making use of this in modelling the wake, it is clear that the greater the distance of the wake behind the blade, the more simply it can adequately be represented, with a consequent saving in computation time. On this basis, for each of the models used here, the wake is divided into a number of regions, these becoming more progressively simplified further below the blade. For the vortex line and vortex ring models, there are three regions, which are defined as near, intermediate, and far. For the vortex lattice model in CAMRAD, there are three regions (representing the inboard wake) applicable to the general case of hover or forward flight, these being defined as near, rolling up (intermediate), and far. However, for the axisymmetric hover case, an additional region, referred to as distant, is included.

2.1 Helical Vortex Lattice Prescribed Wake Model

A vortex lattice model in CAMRAD⁷ based on the prescribed wake geometry of Kocurek and Tangler¹¹ is used here. Finite-length straight-line vortex elements are used for the tip vortices, with an azimuth increment of 15 deg. The inboard wake is divided into three regions of panels, illustrated in Fig. 2 (taken from Ref. 7) for the general case of hover or forward flight, as well as an added distant axisymmetric wake (not shown in Fig. 2) applicable only for the hover case. The same azimuth increment of 15 deg is used for the inboard panels.

In the near wake extending azimuthally for 30 deg directly behind the blade, the inboard vorticity is represented by 15 panels distributed along the blade, with a greater concentration towards the tip, where the greater loading variations occur. Note that in Fig. 2, five equispaced panels are shown. These panels are replaced by a single panel in the far wake. Between the near and far wakes, there is an intermediate, rolling up wake of two panels which change with azimuth increment to represent the transition between the near and far wakes. The rollup and far wake regions extend for a half and five revolutions respectively. By collapsing all the wake panels to trailed finite strength line segments, as used for the tip vortices, a lattice model of the rotor wake is produced.

Beyond the far wake model, a further 30 wake revolutions are added in the form of a distant wake model. In this more simplified axisymmetric model, the tip vorticity is approximated by rectangular vortex sheet panels with axial and spiral components, and the inboard vorticity is approximated by an axial root vortex line.

2.2 Vortex Line Prescribed Wake Model

In the vortex line prescribed wake model, horizontal straight vortex lines perpendicular to the vertical plane of the blade, as shown in Fig. 3, are used for each of the three wake regions. As with the prescribed wake geometry of the vortex lattice model, the vortex line wake geometry is based on the model developed by Kocurek and Tangler from model rotor flow visualization data.

The near wake is represented by a semi-infinite lines attached to, and in the plane of, the blade, with a greater concentration towards the tip. Based on the observations in Kocurek and Tangler's experiments of four well defined tip vortices below the blade, the intermediate wake is represented by two straight infinite vortex lines at each of the corresponding four axial levels. One vortex line is located at the outside boundary of the prescribed contracted wake and represents the strong tip vortex, and the other is located directly beneath the root cutout and represents the inboard vorticity.

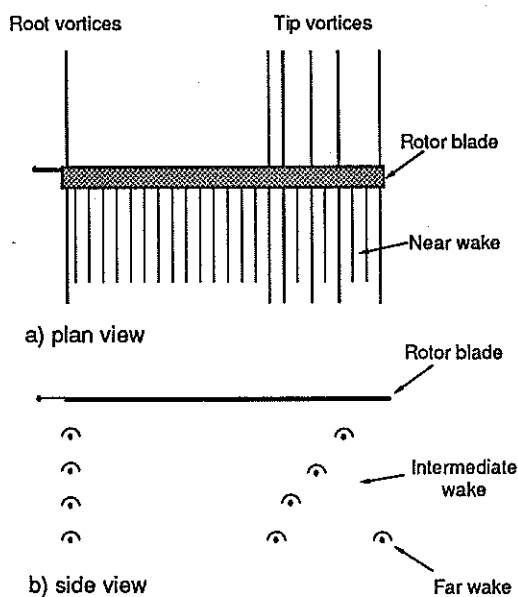


Fig. 3 Vortex line wake model

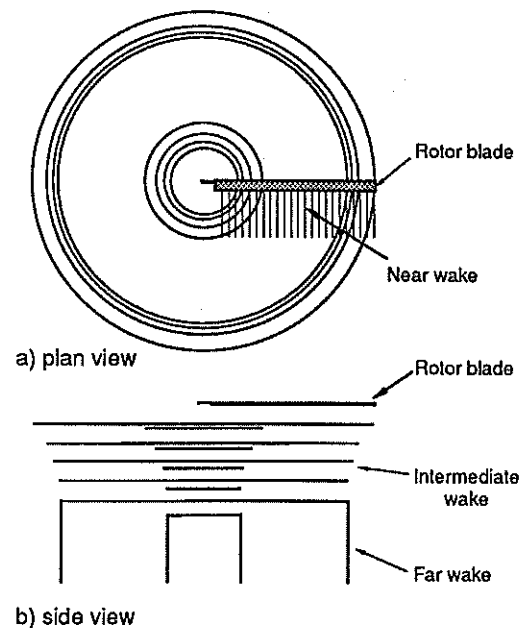


Fig. 4 Vortex ring wake model

Below the intermediate wake region, it is believed that the wake is unstable; the tip vortices undergo viscous dissipation, resulting in wake expansion. To account for this region, which is still close enough to the rotor disc to induce significant inflow, Kocurek and Tangler proposed a vortex ring with radius equal to the rotor radius, axial location at the same level as the fourth tip vortex beneath the rotor, and strength of four times that of the tip vortex. This concept is adopted, but with an infinite straight line replacing the ring in the form of a far wake region, as shown in Fig. 3.

2.3 Vortex Ring Free Wake Model

For both the helical and vortex line wake models, the wake geometry is based on model test results. The problem with this approach is the validity in applying these results to full scale rotors. Parametric studies have shown the high sensitivity of model predictions of inflow velocity, and hence performance, to the positioning of the tip vortices under the blade.⁵ As discussed above, the adoption of a free wake model for hover presents difficulties of convergence when applied to vortex lattice models. However, a simplified model developed by Miller² does not present these difficulties. In Ref. 2, two forms of a simplified model are presented, one using rings, and the other using straight lines in a similar fashion to the one described above. Only the ring model is used here, and the form of this model adopted is described below.

The three wake regions are illustrated in Fig. 4. The near wake, which is identical to the one used for the vortex line method, is represented by semi-infinite vortex lines. The intermediate wake is represented by four axial levels of rings, each level consisting of two rings, the outer one representing the tip vorticity and the inner one representing the inboard vorticity. The radius and axial spacing of each ring is determined by the requirements for equilibrium of the velocities, this being the essence of the free wake method. The far wake is represented by two semi-infinite vortex cylinders with strength determined by the final geometry of the intermediate wake, and positioned one wake spacing below each of the last inner and outer rings of the intermediate region.

3. TEST DATA

The test data for main rotor performance used in this study has been obtained from flight tests of the complete aircraft in the case of the UH-1H¹⁹, Squirrel²⁰, and Wessex¹⁸, and from ground tests of a main rotor attached to a hover test stand facility in the case of the CH-53A¹⁰. For the UH-1H and Squirrel, main rotor performance estimates were derived by subtracting from the total power of the aircraft, allowances of 8% for the tail rotor, 5% for the accessories and transmission, and 2% for aerodynamic interference, giving a net loss of 15%. For the Wessex, Ref. 18 presents only main rotor power, presumably after allowing for similar losses. BHT test results¹¹ for a UH-1D are also included along with the ARDU (Aircraft Research and Development Unit, South Australia) data¹⁹ for a UH-1H.

It is assumed that each blade has a rectangular planform and a NACA 0012 airfoil section. This airfoil is known to be used for the UH-1H and Squirrel, used in modified form for the Wessex/S-58²¹, and assumed by Kocurek et al. for the CH-53A¹⁴. The principal dimensions of each main rotor and the important operating conditions for the test results are summarized in Table 1. Thrust is expressed in coefficient form, C_T , divided by solidity, σ .

4. RESULTS AND DISCUSSION

With each model used here, there is some scope in the selection of certain wake parameters. This is particularly so for the prescribed wake models, mostly because of the uncertainties in applying results based on model scale test data to full scale rotors. For each helicopter, the separate adjustment of these parameters is the usual procedure for matching

Table 1. Basic Test Data

	UH-1H	Squirrel	Wessex	CH-53A
Number of blades, N	2	3	4	6
Solidity, σ	0.0464	0.0534	0.0622	0.114
Radius, R (ft)	24.00	17.54	28.00	36.125
Chord/radius, c/R	0.0729	0.0559	0.0488	0.0600
Linear twist (deg)	-10.9	-12.275	-8.0	-6.0
Root cutout/ R	0.10	0.20	0.16	0.10
Angular velocity (rad/s)	32.99	40.42	22.20	19.27
Blade tip Mach number	0.698	0.630	0.557	0.623
Air density (slug/ft ³)	0.002306	0.002331	0.002378*	0.002378*
Minimum C_T/σ	0.055	0.060	0.070	0.050
Maximum C_T/σ	0.095	0.085	0.095	0.100

* Assumed

model predictions with test results to give a validated model that can be used to investigate the effects of small changes in configuration or operating conditions. To present such contrived predictions of the end result, i.e. performance estimates, without a detailed correlation of intermediate results, e.g. blade loading distribution, simply to demonstrate the merit of each model, is questionable. The main purpose here is to investigate how well each model performs in the absence of individual fine tuning, both for different helicopters and in different thrust regions. Arbitrary choices for parameters still need to be made, but they are done on a uniform basis. Consistency between models is maintained as far as possible, but this objective is somewhat hindered at this stage because each model is coded in a different form. Perhaps the major inconsistency between models is the different representation of airfoil characteristics. In CAMRAD, the airfoil section characteristics are represented in standard C-81 tabular form as functions of angle of attack, α , and Mach number; compressibility effects are therefore effectively incorporated. In the more simplified vortex line and vortex ring models, the characteristics are represented by a constant lift curve slope and a quadratic drag polar ($c_l = 5.73\alpha$ and $c_d = 0.0084 - 0.0102\alpha + 0.384\alpha^2$) without corrections for compressibility. The effect of the important parameters is now discussed.

The prescribed wake geometry model of Kocurek and Tangler, on which both the helical and vortex line models are based, is characterized by expressions defining the axial and radial coordinates of the important tip vortex as functions of thrust coefficient, number of blades, and twist. Equations for the inboard vortex sheet are used by them, without alteration, in the form specified earlier by Landgrebe.¹⁰ The details of both forms of geometry are included in Ref. 6 (Part I). The tip vortex coordinates are described by two-stage axial convection parameters K_1 and K_2 , which are the axial settling rates before and after (respectively) passage of the following blade, and by exponential radial contraction parameters K_3 and K_4 . To improve correlation between performance estimates and test results, it is common to adjust either K_1 (Refs. 5,10) or K_2 (Ref. 8) as a final fine tuning process (see Table 2 for values of K_1 and K_2 at thrust limits; note $K_3 = 4\sqrt{C_T}$ and $K_4 = 0.78$). This is demonstrated following a discussion on the choice of other important parameters.

Tip flow corrections are commonly applied to allow for three-dimensional flow effects at the blade tip. The standard tip loss correction assumes that the blade has drag, but no lift outboard of nondimensional radial station $r = B$. A value for B of 0.985 is suggested by Johnson⁸ for the vortex lattice model in CAMRAD on the basis of the measured position of the rolled up tip vortex at the blade trailing edge. Performance estimates have been found to be very sensitive to this value, depending on proximity of placement to the outer trailing vortex lines. While the proper selection of the tip loss factor in relation to these trailing vortex lines may be important in obtaining

the correct circulation and blade loading distribution, it is considered appropriate to neglect the factor here (i.e. $B = 1$), especially when changes in other parameters are capable of compensating for any differences. The factor is also neglected for the vortex line and vortex ring models. However, for the uniform inflow method in CAMRAD, performance estimates have been found to be fairly insensitive to changes in B , especially at lower thrust values. The standard value of 0.97 is therefore used.

Table 2. Axial settling rates (K_1 , K_2) and blade-vortex axial spacing (h) at minimum and maximum C_T/σ using Kocurek and Tangler wake geometry

	UH-1H		Squirrel		Wessex		CH-53A	
C_T/σ	0.0550	0.0950	0.0600	0.0850	0.0700	0.0950	0.0500	0.1000
K_1	0.0125	0.0244	0.0103	0.0169	0.0165	0.0229	0.0191	0.0365
K_2	0.0415	0.0599	0.0436	0.0569	0.0592	0.0711	0.0708	0.1036
h	0.0392	0.0766	0.0215	0.0353	0.0260	0.0359	0.0200	0.0383

In Table 2, the blade-vortex axial spacing, h , given by $2\pi K_1/N$, is shown for the minimum and maximum thrust. The close spacing, except for the two-bladed UH-1H at the maximum thrust, suggests local flow separation, vortex bursting, and interaction of the vortex with the trailed wake.⁹ Because detailed models for these effects are not yet available, core radius is used in the vortex lattice and vortex ring models as a convenient parameter to account for their combined influence on blade loading and hence performance estimates; in the vortex line method, core size is not used, the effect being incorporated in K_1 . When blade-vortex interaction is suspected, a larger (burst) core radius is used after the interaction for the vortex lattice model, and both before and after for the simpler vortex ring model. A burst core radius (nondimensionalized by R) of 0.05 is suggested by Johnson (Ref. 8, p. 209), and an unburst radius of 10% of c/R is typically assumed (Ref. 16, p. 536), resulting here in values between 0.005 and 0.007 (from Table 1). Because results were found to be fairly insensitive to significant changes in the unburst value, 0.005 was assumed for all cases. However, results were found to be sensitive to changes in the burst value,

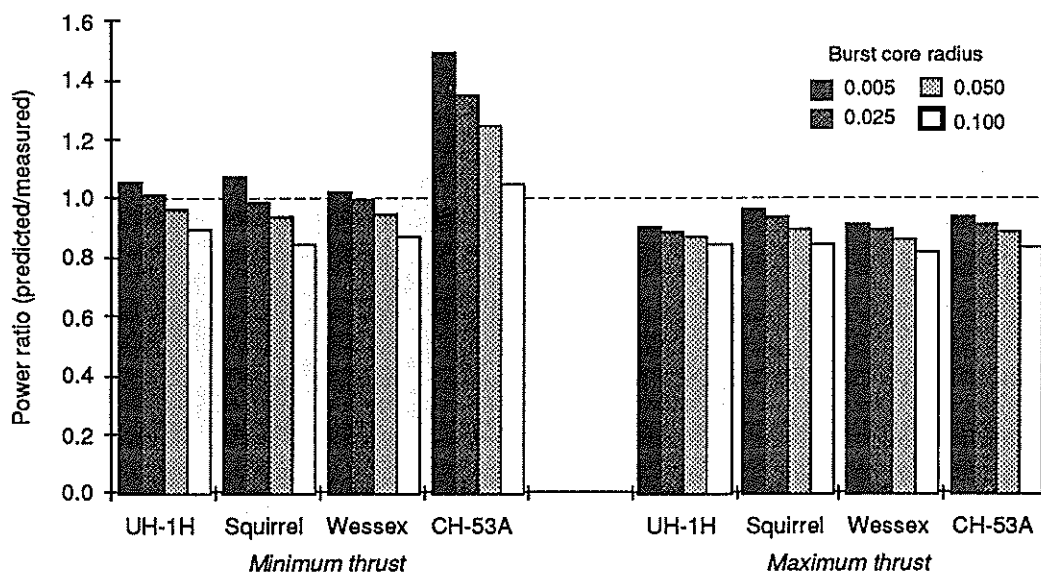


Fig. 5 In vortex lattice model, effect on hover performance of burst core radius

and these are shown in Fig. 5 for the vortex lattice model. The power estimates are presented in the form of the ratio of model predictions to smoothed test results. Note that the lower burst core radius, set to the unburst value of 0.005, corresponds to the case of no core bursting, which is assumed to apply for the UH-1H at maximum thrust. For the other helicopters at maximum thrust, a similar power ratio of 0.9 is given by assuming the burst core radius of 0.05 suggested above. By also assuming the same value at the lower thrust, all performance predictions in Fig. 5 are about 5 to 15% optimistic (i.e. lower than the test data), except for the CH-53A at the minimum thrust, where the prediction is about 25% pessimistic.

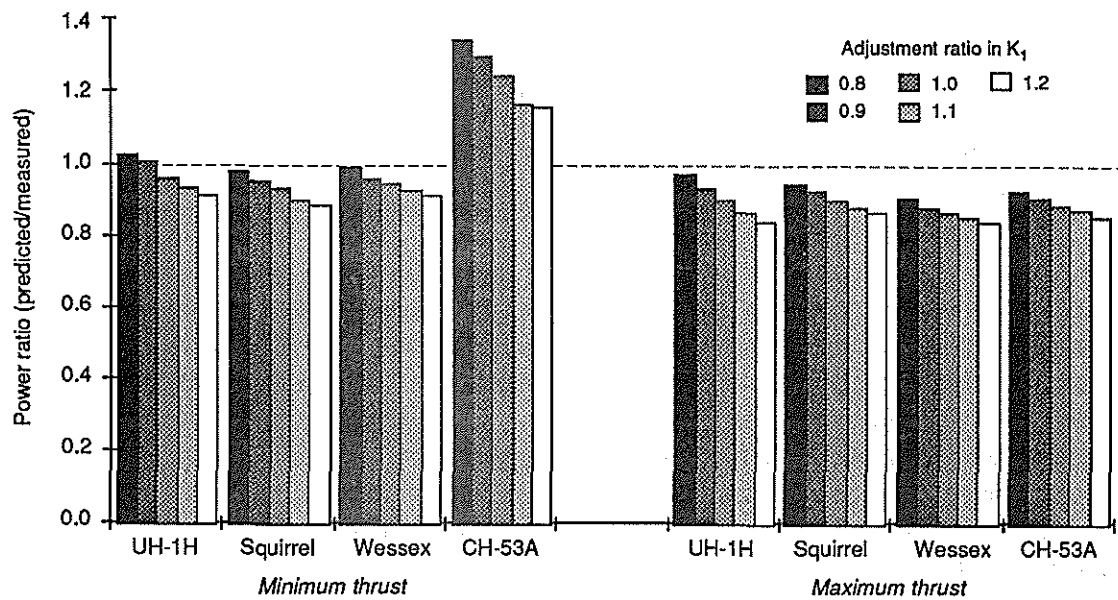


Fig. 6 In vortex lattice model, effect on hover performance of tip vortex axial settling rate (K_1) before passage of following blade

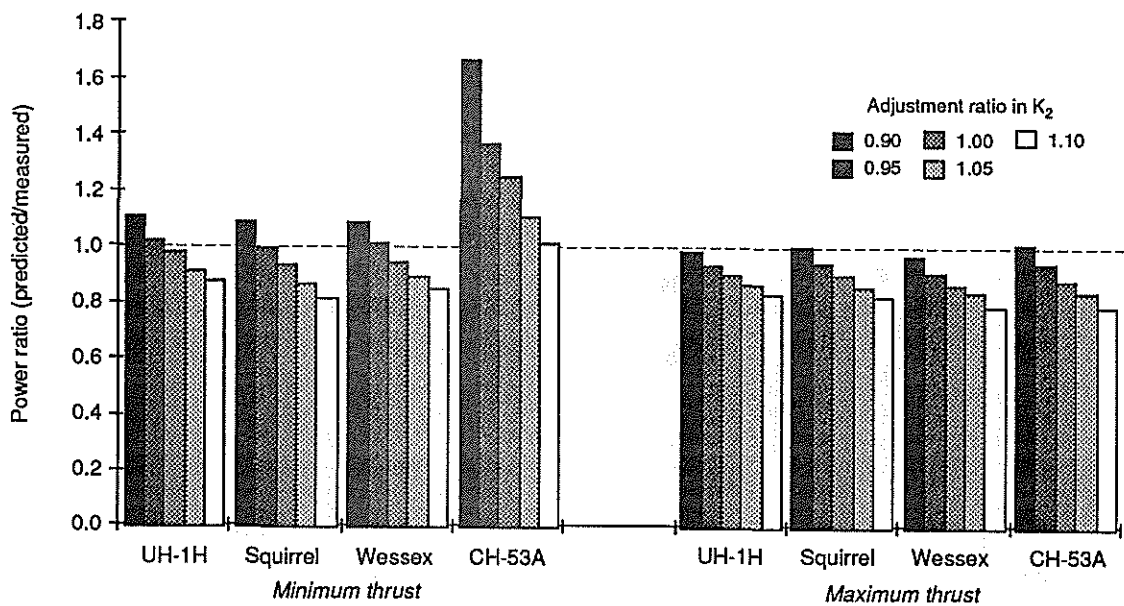


Fig. 7 In vortex lattice model, effect on hover performance of tip vortex axial settling rate (K_2) after passage of following blade

For the vortex lattice model, sensitivity of power estimates to adjustments in K_1 and K_2 are shown in Figs. 6 and 7 respectively at the minimum and maximum thrusts for each helicopter selected. The adjustments are given in the form of a ratio of the adjusted parameter to that given by Kocurek and Tangler's model rotor experimental data. The unadjusted performance predictions correspond to the middle column of each group where the parameter ratio is unity. Generally, a 5% change in power is given by adjustments in K_1 of about 20% and in K_2 of about 5%, except for the CH-53A at the minimum thrust, where these adjustments give a change in power of about 10-15%. The greater cumulative effect of changes in the far wake convection parameter K_2 suggest that it be adjusted in preference to K_1 . To match the flight data would require a reduction in K_2 of about 5% at minimum thrust (increase of 10% for CH-53A) and about 10% at maximum thrust, which is similar to reductions suggested by Johnson.⁸⁻⁹

For the vortex line model, parametric studies have shown that the sensitivity of power estimates to K_1 alone is sufficient to account for differences between predictions and test results for the UH-1H. Further parametric studies are therefore not considered necessary. Because the wake geometry is calculated, rather than prescribed, in the vortex ring model, there is less scope for parameter adjustment, core radius being the only main one. Sensitivity studies on the choice of this parameter are not presented, being similar to those given in Fig. 5 for the vortex lattice model.

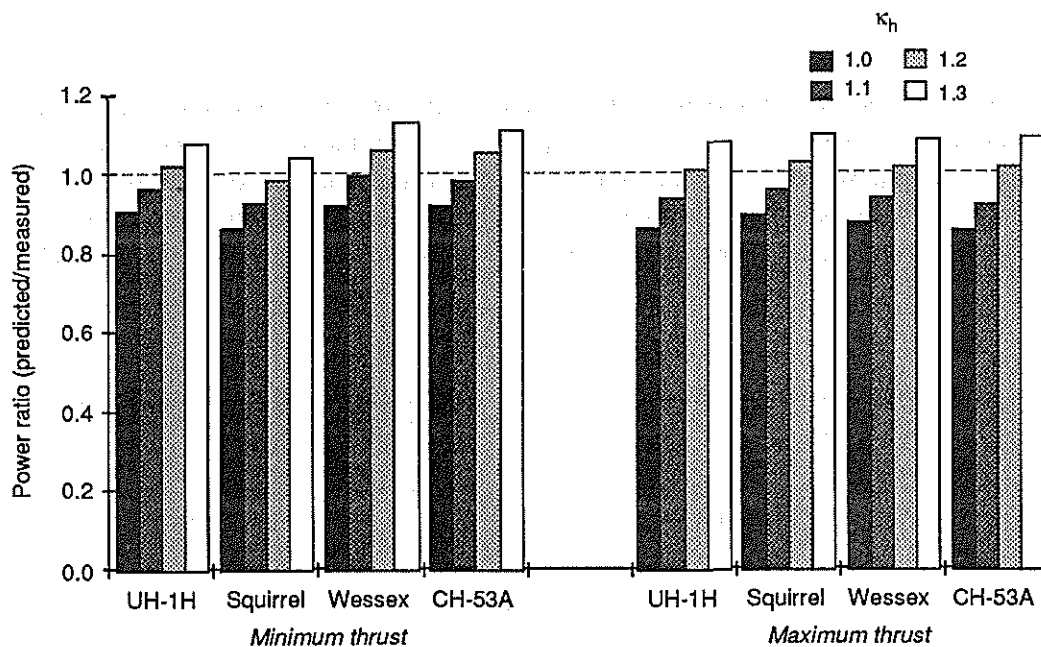


Fig. 8 In uniform inflow model, effect on hover performance of induced velocity factor (κ_h)

With the uniform inflow method, induced power is mostly underestimated, which has been attributed to the inadequate modelling of a number of effects that include nonuniform inflow, tip losses, swirl, and blockage.⁷ An empirical 'induced velocity' correction factor, κ_h , in the range 1.1-1.25, is usually used to improve correlation for total power. Fig. 8 shows the effect of a range of values for κ_h , including the case of 'no correction', i.e. $\kappa_h = 1$, where the results are 10-15% optimistic. With $\kappa_h = 1.2$ assumed uniformly, the results are 1-2% pessimistic at maximum thrust, and from 2% optimistic to 5% pessimistic at minimum thrust.

For each helicopter and model, Figs. 9-12 show the performance estimates in the form of power coefficient divided by solidity (C_p/σ) for the complete range of C_T/σ . The parameters K_1 and K_2 , used in the vortex lattice model, have not been adjusted from the values given in Table 2 by the model rotor data, mainly because a uniform correction is not possible. The above standard

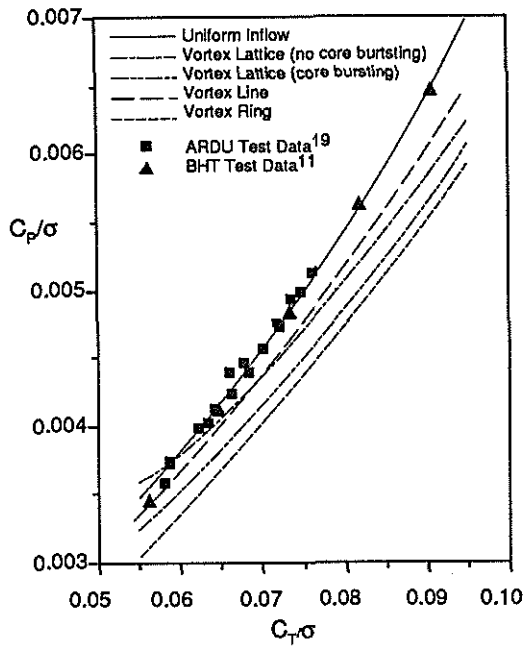


Fig. 9 Main rotor hover performance for UH-1H

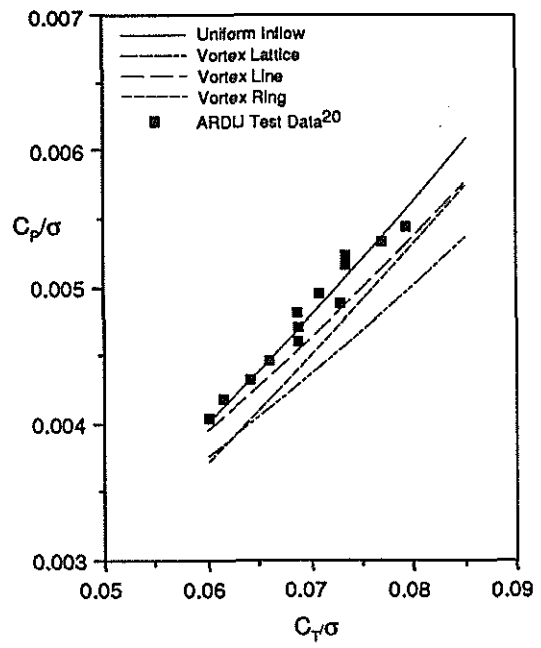


Fig. 10 Main rotor hover performance for Squirrel

unburst and burst core radii of 0.005 and 0.05 respectively are assumed in the vortex lattice and vortex ring models. However, for the UH-1H over the whole thrust range, the vortex line and vortex ring results assume no core bursting, while the vortex lattice results are presented both with and without core bursting. In the vortex line results, core bursting is represented by an increase of 25% in K_7 . The uniform inflow results are shown with $\kappa_h = 1.2$ assumed uniformly.

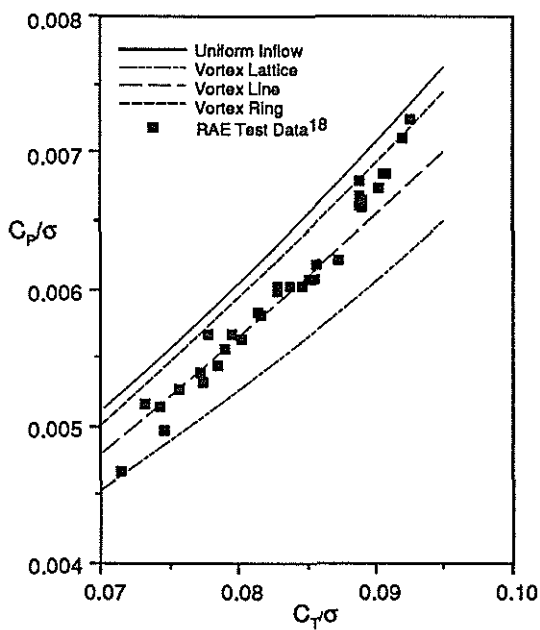


Fig. 11 Main rotor hover performance for Wessex

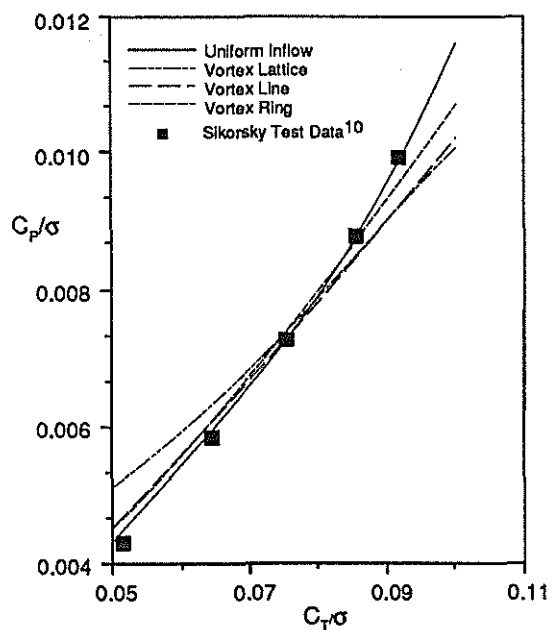


Fig. 12 Main rotor hover performance for CH-53A

In the absence of individual fine tuning, performance estimates given by the three nonuniform inflow wake models show wide variations, which contrast with the consistently good estimates provided by the uniform inflow method. It is interesting to note that the success of momentum methods has been attributed in Ref. 11 firstly to the compensating effect of errors in the inflow distribution and secondly through judicious application of empiricisms by experienced users. While agreeing with the former, the evidence here suggests that the latter appears far more applicable to the wake modelling methods.

The usefulness of each model in predicting the intermediate result of blade load distribution is demonstrated in Fig. 13 for the S-58 (equivalent to Wessex). There is considerable scatter in the experimental results of Scheiman,²¹ which may be due to the unsteady, unsymmetric wake applicable to a hovering helicopter. The test results in Fig. 13 were obtained by taking the mean value at each radial station over 24 azimuth positions, with the scatter shown by the 12.5 and 87.5 percentiles. Because there were small variations of helicopter weight in the tests, the mean value was assumed; the deviation from this mean of $\pm 2.6\%$ would result in a similar error in the loads. The agreement given by each of the three wake models is seen to be good, lying within the experimental scatter for the outer 40% of blade radius. The agreement for the inner portion of the blade is reasonable considering the simple models used to represent the inboard vorticity. As expected, it is clear that the uniform inflow method does not represent the load distribution as well as the wake methods.

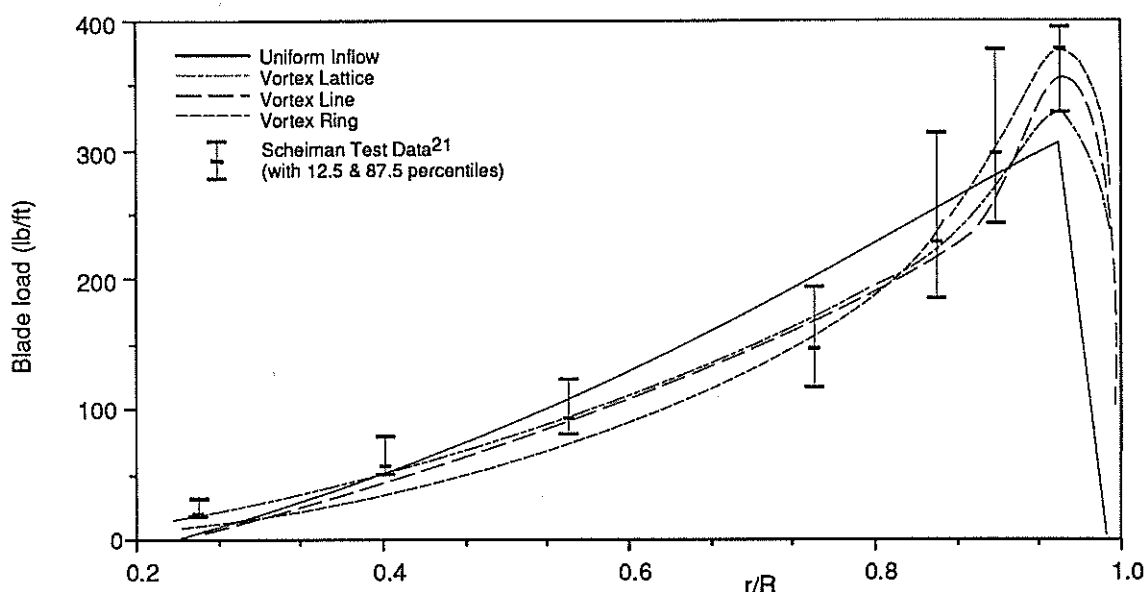


Fig. 13 Blade load distribution for S-58

5. CONCLUDING REMARKS

Performance estimates obtained using three nonuniform wake models and a uniform inflow method based on momentum theory have been compared with test data for four helicopters. The study has shown that while it is usually possible for an experienced user to individually fine tune the nonuniform inflow methods for each case to match predictions with test results, none of these methods can be used at present with confidence for accurate prediction (within $\pm 5\%$), where experimental data are unavailable. Though the uniform inflow method does provide consistently good estimates, at least for the cases shown here, it does not give good intermediate results, e.g. for blade load distribution. Given the problem of providing estimates without test data, and with only the models used here, a suggested strategy would be to first use the uniform inflow method to provide total power estimates, and then to fine tune one of the other

methods to match these results so that more accurate estimates of the intermediate results can be obtained. In order to overcome the major inconsistency between the wake models, it is planned to incorporate the vortex line and vortex ring models into CAMRAD. The detailed tabular representation of the two-dimensional airfoil characteristics, which include compressibility effects, will then be available to these simpler models.

References

1. K. R. Reddy, The vortex flow field generated by a hovering helicopter, **Proceedings of the 7th Australasian Conference on Hydraulics and Fluid Mechanics**, Brisbane, Australia, pp. 553-556, Aug. 1980.
2. R. H. Miller, A simplified approach to the free wake analysis of a hovering rotor, **Proceedings of the Seventh European Rotorcraft and Powered Lift Aircraft Forum**, Garmisch-Partenkirchen, W. Germany, Paper No. 2, Sept. 1981; also, **Vertica**, Vol. 6, pp. 89-95, 1982.
3. C. R. Guy, M. J. Williams, and N. E. Gilbert, ASW helicopter/sonar dynamics mathematical model, **Proceedings of the Sixth European Rotorcraft and Powered Lift Aircraft Forum**, Bristol, England, Paper No. 45, Sept. 1980.
4. M. J. Williams and A. M. Arney, Helicopter hover performance estimation - comparison with UH-1H Iroquois flight data, **ARL-AERO-TM-377**, April 1986.
5. K. R. Reddy, The effect of rotor wake geometry variation on hover induced power estimation for a UH-1H Iroquois helicopter, **ARL-AERO-TM-384**, Oct. 1986.
6. W. Johnson, A comprehensive analytical model of rotorcraft aerodynamics and dynamics, Parts I, II, and III, **NASA TM-81182,3**, and 4, June/July 1980.
7. W. Johnson, Development of a comprehensive analysis for rotorcraft - I. Rotor model and wake analysis, **Vertica**, Vol. 5, pp. 99-129, 1981.
8. W. Johnson, Development of a comprehensive analysis for rotorcraft - II. Aircraft model solution procedure and applications, **Vertica**, Vol. 5, pp. 185-216, 1981.
9. W. Johnson, Assessment of aerodynamic models in a comprehensive analysis for rotorcraft, **NASA TM-86835**, Oct. 1985.
10. A. J. Landgrebe, The wake geometry of a hovering helicopter rotor and its influence on rotor performance, **Journal of the American Helicopter Society**, Vol. 17, No. 4, pp. 3-15, Oct. 1972.
11. J. D. Kocurek and J. L. Tangler, A prescribed wake lifting surface hover performance analysis, **Proceedings of the 32nd Annual National V/STOL Forum of the American Helicopter Society**, Washington, D.C., Preprint No. 1001, May 1976.
12. R. A. Ormiston, Comparison of several methods for predicting loads on a hypothetical helicopter rotor, **Journal of the American Helicopter Society**, Vol. 19, No. 4, pp. 2-13, Oct. 1974; also, **Proceedings of the AHS/NASA Ames Specialists' Meeting on Rotorcraft Dynamics: NASA SP-352**, pp. 284-302, Feb. 1974.
13. F. D. Harris, Rotary wing aerodynamics - historical perspective and important issues, **Proceedings of the AHS Sponsored National Specialists' Meeting on Aerodynamics and Aeroacoustics**, Arlington, Texas, Feb. 1987.
14. J. D. Kocurek, L. F. Berkowitz, and F. D. Harris, Hover performance methodology at Bell Helicopter Textron, **Proceedings of the 36th Annual Forum of the American Helicopter Society**, Washington, D.C., Preprint No. 80-3, May 1980.
15. R. B. Gray, On the motion of the helical vortex shed from a single-bladed hovering helicopter rotor and its application to the calculation of the spanwise aerodynamic loading, **Princeton Univ. Aeronautical Eng. Dept. Report No. 313**, Sept. 1955.
16. W. Johnson, **Helicopter Theory**, Princeton University Press, 1980.
17. D. B. Bliss, D. A. Wachspress, and T. R. Quackenbush, A new approach to the free wake problem for hovering rotors, **Proceedings of the 41st Annual Forum of the American Helicopter Society**, Ft. Worth, Texas, pp. 463-477, May 1985.
18. C. Young, The representation of the helicopter rotor wake in hover, **RAE Tech. Report 82121**, Dec. 1982.
19. Flight test report: UH-1H Iroquois performance evaluation, **ARDU Report No. TS 1631**, Nov. 1976.
20. AS-350B Squirrel performance definition and validation, **ARDU Report No. TS 1687**, to be published.
21. J. Scheiman, A tabulation of helicopter rotor-blade differential pressures, stresses, and motions as measured in flight, **NASA TM X-952**, March 1964.